Computational Biology and Chemistry 64 (2016) 237–249

Contents lists available at ScienceDirect

Computational Biology and Chemistry

journal homepage: www.elsevier.com/locate/compbiolchem

Research article

# Assembly of ligands interaction models for glutathione-*S*-transferases from *Plasmodium falciparum*, human and mouse using enzyme kinetics and molecular docking

Mohammed Nooraldeen Al-Qattan[a,*], Mohd Nizam Mordi[b], Sharif Mahsofi Mansor[b]

[a] *Faculty of Pharmacy, Philadelphia University, 19392 Jordan*
[b] *Centre For Drug Research, Universiti Sains Malaysia. Gelugor 11700 Penang, Malaysia*

ARTICLE INFO

*Article history:*
Received 4 June 2015
Received in revised form 8 July 2016
Accepted 16 July 2016
Available online 25 July 2016

*Keywords:*
Enzyme kinetics
Molecular docking
*Pf*GST
hGSTP1
mGSTM1

ABSTRACT

*Background:* Glutathione-*s*-transferases (GSTs) are enzymes that principally catalyze the conjugation of electrophilic compounds to the endogenous nucleophilic glutathione substrate, besides, they have other non-catalytic functions. The *Plasmodium falciparum* genome encodes a single isoform of GST (*Pf*GST) which is involved in buffering the toxic heme, thus considered a potential anti-malarial target. In mammals several classes of GSTs are available, each of various isoforms. The human (human GST Pi-1 or hGSTP1) and mouse (murine GST Mu-1 or mGSTM1) GST isoforms control cellular apoptosis by interaction with signaling proteins, thus considered as potential anti-cancer targets. In the course of GSTs inhibitors development, the models of ligands interactions with GSTs are used to guide rational molecular modification. In the absence of X-ray crystallographic data, enzyme kinetics and molecular docking experiments can aid in addressing ligands binding modes to the enzymes.
*Methods:* Kinetic studies were used to investigate the interactions between the three GSTs and each of glutathione, 1-chloro-2,4-dinitrobenzene, cibacron blue, ethacrynic acid, *S*-hexyl glutathione, hemin and protoporphyrin IX. Since hemin displacement is intended for *Pf*GST inhibitors, the interactions between hemin and other ligands at *Pf*GST binding sites were studied kinetically. Computationally determined binding modes and energies were interlinked with the kinetic results to resolve enzymes-ligands interaction models at atomic level.
*Results:* The results showed that hemin and cibacron blue have different binding modes in the three GSTs. Hemin has two binding sites (A and B) with two binding modes at site-A depending on presence of GSH. None of the ligands were able to compete hemin binding to *Pf*GST except ethacrynic acid. Besides bind differently in GSTs, the isolated anthraquinone moiety of cibacron blue is not maintaining sufficient interactions with GSTs to be used as a lead. Similarly, the ethacrynic acid uses water bridges to mediate interactions with GSTs and at least the conjugated form of EA is the true hemin inhibitor, thus EA may not be a suitable lead.
*Conclusions:* Glutathione analogues with bulky substitution at thiol of cysteine moiety or at γ-amino group of γ-glutamine moiety may be the most suitable to provide GST inhibitors with hemin competition.



## 1. Background

Glutathione-*s*-transferase (GST) is bi-substrate detoxification enzyme involved mainly in catalyzing the conjugation of xenobiotics bind at hydrophobic-site (H-site) to endogenous glutathione substrate bind at glutathione-site (G-site). Besides, other catalytic functions were reported for GSTs including isomerization and peroxidase activities. While the non-catalytic functions of GSTs include carriage of small organic molecules and interaction with signaling proteins involved in cellular apoptosis (Hayes et al., 2005; Townsend, 2007; OAKLEY, 2011). Therefore, it is not surprising that inhibition of GSTs has various medicinal applications as anthelmintic, anti-parasitic, and anti-cancer (Brophy and Barrett, 1990; McTigue et al., 1995; Harwaldt et al., 2002; Ruzza et al., 2009).

In mammals, about 7 classes of cytosolic GSTs were discovered, each involves several isoforms (Nebert and Vasiliou, 2004; Mannervik et al., 2005; Frova, 2006). Of the most medicinally

* Corresponding author.
*E-mail address:* mohammed_alqattan@yahoo.com (M.N. Al-Qattan).

http://dx.doi.org/10.1016/j.compbiolchem.2016.07.007
1476-9271/

relevant mammalian GST isoforms is the human Pi-1 (hGSTP1). The hGSTP1 is involved in detoxification of chemotherapies, thus overexpressed in resistant cancer cells (Parker et al., 2008; Kalinina et al., 2012). The human isoform Mu-1 (hGSTM1) shares 78% sequence similarity with mouse isoform (mGSTM1) according to BLAST search over human genome. Both of mGSTM1 and hGSTP1 inhibit the apoptotic stress kinase pathway by interaction with signal regulating kinase-1 (Cho et al., 2001) and its C-Jun N-terminal Kinase (JNK) substrate (Adler et al., 1999; Townsend and Tew, 2003; Townsend et al., 2005; Laborde, 2010; DE Luca et al., 2012), respectively.

The genome of *Plasmodium falciparum* encodes a single isoform of cytosolic GST (Harwaldt et al., 2002; Liebau et al., 2002) as well as a membrane bound GST(Lisewski et al., 2014). The *Plasmodium falciparum* cytosolic GST (*Pf*GST) is involved in capturing or degradation of free hemin that fails to be polymerized into hemozoin (Egan et al., 2002; Liebau et al., 2005; Liebau et al., 2009), thus *Pf*GST is overexpressed in chloroquine resistant strains for the parasite (Srivastava et al., 1999; Deharo et al., 2003). The *Pf*GST is highly expressed in the parasite and constitutes about 3% of the total extractable proteins (Harwaldt et al., 2002). The structure of *Pf*GST is novel and cannot be assigned to any of the known GST classes (Liebau et al., 2002). Therefore, *Pf*GST was considered as an attractive target for antimalarial design (Harwaldt et al., 2002; Fritz-Wolf et al., 2003). The medicinal significance of targeting *Pf*GST was approved biochemically (Srivastava et al., 1999; Deponte and Becker, 2005), in silico by gene knock-out study (Fatumo et al., 2009), and by stage-specific metabolic network analysis (Huthmacher et al., 2010). Yet no lead molecule has been developed to inhibit *Pf*GST and intervene its parasito-protective hemin buffering.

The structure-based rational design of GST inhibitor requires a lead molecule of defined interaction model with GST. X-ray crystallographic structures are available for several ligands (substrates and non-substrates) in complex with hGSTP1 (Ji et al., 1997; Oakley et al., 1997a; Oakley et al., 1997c; Prade et al., 1997; Oakley et al., 1999; Federici et al., 2009; Parker et al., 2011), however fewer structures are available for *Pf*GST (Fritz-Wolf et al., 2003; Perbandt et al., 2004; Hiller et al., 2006) and none for mGSTM1.

X-ray crystallography is the technique of choice to determine protein-ligand complex, however, the dynamic behavior of the ligand is usually averaged by this technique. For example ligand may flip between sub-sites within the protein binding pocket which can be occasionally observed upon using different crystallization techniques (Danley, 2006; Davis et al., 2008). For example, glutathione-ethacrynic acid (GS-EA) conjugate in hGSTP1 was observed to flip between two binding modes (PDBIDs 3GSS and 11GS) that was recognized by using different techniques of introducing ligand to protein crystal (crystal soaking vs co-crystallization) (Oakley et al., 1997b; Oakley et al., 1997c). Similarly, the affinity of ligand toward *Pf*GST was affected by composition of the crystallization solution being used (Fritz-Wolf et al., 2003). The most suitable method to determine the dynamic behavior of a ligand at enzyme binding site is the kinetic study. The results of enzyme kinetic studies can be discussed with results from molecular docking to provide 3D molecular models about enzyme-ligand interactions. The models can provide valuable assist for structure-based inhibitor design especially for ligands of unavailable crystal structures.

In this study, the interactions between common GST ligands (including substrates and inhibitors) and each of *Pf*GST, hGSTP1 and mGSTM1 were investigated by enzyme kinetic as well as molecular docking studies. The kinetic and computational results were used to conclude GST-ligands interaction models with respect to binding modes and affinities.

## 2. Materials and methods

The glutathione (GSH) and 1-chloro-2,4-dinitrobenzene (CDNB) were from Nacalai Tesque (Japan); the *S*-hexyl glutathione (GSX), hemin and protoporphyrin IX (protoIX) were from Sigma Aldrich (China); the cibacron blue from Calbiochem (Canada); the ethacrynic acid (EA) from Santa Cruz (USA); DMSO and HEPES from Merck (Germany); and Phosphate salts from Merk (Germany).

### 2.1. Preparation of GSTs, buffers and stocks of substrates and inhibitors

All of *Pf*GST, hGSTP1, mGSTM1 enzymes have been heterologously expressed and purified as described elsewhere (Al-Qattan et al., 2015). The buffers used for enzymatic assay were 100 mM HEPES buffer (pH 6.5) for *Pf*GST (Harwaldt et al., 2002), while 100 mM potassium phosphate buffer (pH 6.5) was used for hGSTP1 and mGSTM1 (Habig et al., 1974). GSH stock solution of 5 mM was prepared in 100 mM phosphate or HEPES buffers and the pH was adjusted to 6.5 using either KOH or NaOH, respectively. CDNB stock solution of 20 mM was prepared in absolute ethanol (Habig et al., 1974). The buffers were used as solvents for GSX and CB, while DMSO was used for EA, hemin and protoIX. Stock solutions were prepared in fresh before use and kept away from light on ice blocks during assays.

### 2.2. Measurement of initial enzyme velocity and determination of kinetic constants

The enzymes activities regarding CDNB conjugation were measured using the extinction coefficient of GS-DNB conjugate at 340 nm ($9.6\,mM^{-1}\,cm^{-1}$) (Habig et al., 1974). The Thermo Scientific™ Multiskan GO UV/V microplate reader was used to measure the absorbance over 20 min while maintain temperature at 26 °C (Habig et al., 1974; Harwaldt et al., 2002).

The initial enzyme velocity ($v_i$) was measured by fitting fourth polynomial function to the GS-DNB product progress curve using Data Curve Fit Creator Add-in to Excel (http://www.srs1software.com/DataCurveFitCreator.aspx the link was available in 3 June 2015) before taking the first derivative of the function (Claro, 2000).

The standard reaction of GST assay contained 1 mM of GSH and 1 mM of CDNB and in 100 mM potassium phosphate or HEPES buffers (pH 6.5). The reaction was started with addition of enzyme. In order to determine the substrates binding modes, $v_i$ was measured at variable concentrations of GSH and CDNB, then used to fit three equations representing random-ordered, compulsory-ordered and Ping-Pong mechanisms (Copeland, 2000). In the course of determining binding modes and $K_i$ values for inhibitors, the $v_i$ as well as the concentrations of substrate and inhibitors were used to fit three equations representing competitive, non-competitive and uncompetitive inhibitions (Copeland, 2000). The $K_i^{GSH}$ and $K_i^{CDNB}$ were determined by varying the inhibitor concentration as well as the concentrations of GSH and CDNB, respectively. Finally, the deduced constants of $V_{max}$, $K_m$, $K_i$, and $\alpha$ factor from the fitted equation were used to draw Lineweaver-Burk plot (i.e. double-reciprocal plot for $v$ and $[S]$) . The extent of interactions between two inhibitors at enzyme binding sites were determined by measuring $v_i$ in the standard reaction while simultaneously varying the concentrations of two inhibitors. The data used to fit double inhibitor equation to deduce interaction factor and respective dissociation constant for each inhibitor. (Copeland, 2000; Leskovac, 2003). The interaction between HEPES and hemin was studied using inactive tetrameric form of *Pf*GST. *Pf*GST tetramer was prepared by incubation in GSH deprived potassium phosphate buffer pH 6.5 at 4 °C overnight to enhance

tetramerization (Liebau et al., 2005). Before reaction initiation, the enzyme was pre-incubated with the respected concentration of HEPES for 7 min at room temperature (27–28 °C).

### 2.3. Molecular docking and energy optimization

Molecular docking were performed using AUTODOCK4.2 (Huey et al., 2007). The *Pf*GST receptor files used for docking were 1Q4J for hemin ((Harwaldt et al., 2002)) and 2AAW for other ligands. While receptor files for hGSTP1 were 8GSS for hemin, 20GS for cibacron, 3GSS for EA. Since the docking site was away from the dimeric interface, monomeric form of the receptors was used. The apo form of receptors was used for docking all ligands except hemin where two docking experiments performed in presence and absence of GSH at G-site. The ligand was prepared starting from SMILE code converted into 3D structure and optimized by MMFF94s using Obabel (from OpenEye). All ligands bonds are considered rotatable during docking except peptide bonds, double bonds and bonds involved in aromatic rings. The grid box was adjusted to cover both of G- and H-sites and include a molecule of GSH in case of hemin docking. The docking parameter files were set to default values except in the exhaustive search which uses population size of 250, maximum number of generations of 40,000, and number of runs of 100. All receptor, ligand and docking files were prepared by AUTODOCK Tools. The Cartesian coordinate optimization and energy calculation for protein and protein-ligand complex was performed using SZYBKI (from OpenEye) with MMFF94. Chimera 1.7 was used for structural alignment or superposition using 'best-aligning pair of chains' option including secondary structure score.

## 3. Results and discussion

With respect to docking experiments, several trials were made using dimeric form of GST, however, it expand the searching space and led to ligands being traped in probable local minima. Ligands with several polar groups (such as cibacron blue) tend to deoccupy ligand binding sites at first monomer toward the dimeric interface, thus increasing solvent accessible surface for the ligand. Therefore, the search space was compromised through considering monomeric form of GST during docking.

The docked conformation (pose) was selected from the docking results based on criteria that inlcude: lower iteractions energy, lower water accessible surface area, lower bumping with amino acids from second GST monomer, as well as similarity to available crystal conformations. For example, the docked conformation of cibacron blue against hGSTP1 was selected to provide fit for anthraquinone moiety with crystal data. On the other hand, the conformations which docked close to the dimeric interface and bumps with atoms from second monomer were ommited during cibacron blue docking to *Pf*GST. With repsect to hemin docking to hGSTP1, the conformation which provides interaction of carboxylic group with the portein was selected over the next energy ranked conformation in which the carboxylic group is directed toward the solution, although the difference in energy score between the two conformations was less than 0.25 Kcal/Mol.

Following ligand docking, the selected poses were subjected to local minimization with more precise force-field which measures entropic parameters and solvent effect. This step was to further improve conformational ligand fit and to obtain better estimation of final energy compared to semi-empirical force field of AUTODOCK 4.2 (i.e. The estimated free energy of binding)

The experimental determination of kinetic constants and inhibitory modes was made by curve fitting to the kinetic data. The fitting was manually checked, and only the modes which provide lowest standard errors, errhigher confidence interval and best fitness measured by $R^2$ was chosen.

### 3.1. Determination of $K_m^{GSH}$ and $K_m^{CDNB}$ for Pf*GST, hGSTP1, and mGSTM1*

The affinities toward GSH and CDNB substrates were used to confirm the functionality of enzymes. With respect to hGSTP1, the values of $K_m^{GSH}$ (0.42 mM) and $K_m^{CDNB}$(1.6 mM) were slightly higher than the reported values (0.18 and 0.77 mM, respectively) (Manoharan et al., 1992; Zimniak et al., 1994; Huang et al., 2008). The difference can be attributed to lower activity of hGSTP1 which adds linearity to product progress curve used for polynomial fitting. With regard to mGSTM1, both of $K_m^{GSH}$ and $K_m^{CDNB}$ values were equal to 0.26 mM, which are close to the values reported for Mu class of mouse (0.48 and 0.38 mM, respectively) (Medh et al., 1991), as well as human Mu-1 isoform (Patskovsky et al., 1999; Patskovsky et al., 2000) which shows 78% sequence similarity to mGSTM1.

Using HEPES buffer, the affinity of GSH toward *Pf*GST ($K_m^{GSH}$) was determined to be 0.174 mM which was consistent with the reported value (0.164 mM) (Harwaldt et al., 2002). However, the *Pf*GST activity reduced when potassium phosphate buffer was used; which introduced a lag phase at the beginning of reaction (see Supplementary material, Figure I). The lag phase was more pronounced at GSH < 1 mM and interferes with measurements of initial enzyme velocity. Low concentrations of GSH and HEPES were reported to predominate the inactive tetrameric form of *Pf*GST (Harwaldt et al., 2002; Tripathi et al., 2007; Liebau et al., 2009). The affinity of CDNB toward *Pf*GST ($K_m^{CDNB}$) was determined to be ~10 mM. The *Pf*GST was reported to have very low specific activity toward the co-substrate CDNB ($K_m^{CDNB}$ > 10 mM), which is 50–100 times lower than Alpha, Pi, and Mu classes (Harwaldt et al., 2002; Liebau et al., 2005). The summary of determined and reported $K_m$ values are shown in Table 1.

### 3.2. Determination of the mechanisms for GSH and CDNB mode of binding

GSTs are bisubstrate enzymes which catalyze bond formation between endogenous substrate of GSH at G-site and exogenous hydrophobic substrate at H-site of the enzyme. The substrates binding mechanism can give clues about the possible interaction

**Table 1**
The $K_m$ constants (mM) for GSH and CDNB toward PfGST, hGSTP1, mGSTM and hGSTM1.

| ENZYME | EXPERIMENTAL | | LITERATURE | | |
|---|---|---|---|---|---|
| | $K_m^{GSH}$ | $K_m^{CDNB}$ | $K_m^{GSH}$ | $K_m^{CDNB}$ | REFERENCES |
| *Pf*GST | 0.174 ± 0.002 | 9.8 ± 2.6 | 0.164 ± 0.02 | >10.00 | Harwaldt et al. (2002), Liebau et al. (2005) |
| hGSTP1 | 0.42 ± 0.13 | 1.57 ± 0.24 | 0.18 ± 0.07 | 0.77 ± 0.16 | Manoharan et al. (1992), Zimniak et al. (1994), Huang et al. (2008) |
| mGSTM1 | 0.26 ± 0.03 | 0.26 ± 0.06 | 0.48 (*) | 0.38 (*) | Medh et al. (1991) |
| hGSTM1 | NA | NA | 0.14 | 0.31 | Patskovsky et al. (1999), Patskovsky et al. (2000) |

Note: All experiments were performed minimally as duplicates.
(*) Means the values are for nonspecific Mu class members, and NA means no available measurements.

**Table 2**
The binding modes of GSH and CDNB in PfGST, hGSTP1, and mGSTM1. The values of dissociation constants for GSH and CDNB as well as the interaction factor were obtained from the respected fitted equations.

| GSTs | (mM) | (mM) | α factor | Mode |
|---|---|---|---|---|
| *Pf*GST | 0.177 ± 0.01 | 5.08 ± 0.9 | – | Compulsory-ordered |
| hGSTP1 | 0.145 ± 0.04 | 0.4 ± 0.11 | 2.6 ± 1 | Random-ordered |
| mGSTM1 | 0.33 ± 0.11 | 0.24 ± 0.06 | 0.65 ± 0.28 | Random-ordered |

between the binding sites and whether one substrates enhance or inhibit binding of the other. Previous studies showed that binding of GSH and CDNB to GSTs follows random ordered mechanism (Jakobson et al., 1979; Schramm et al., 1984; Ivanetich and Goold, 1989; Ivanetich et al., 1990), however, others suggest it is ordered with GSH binding first (Pickett and Lu,1989; Armstrong, 1991).

The kinetic results showed that only *Pf*GST can fit to compulsory-ordered equation (Table 2) by assuming the formation of conjugation bond – between GSH and CDNB – is the rate limiting step for the reaction. The dissociation constants for GSH and CDNB were 0.17 and 5.0 mM, respectively, which are consistent with the observed $K_m$ values. Accordingly, GSH may bind first to *Pf*GST, thus mediates stabilizing interactions with the next coming CDNB, however, GSH does not bind to *Pf*GST-CDNB complex. The observation could explain the low specific activity or affinity of *Pf*GST toward CDNB (Harwaldt et al., 2002; Liebau et al., 2002), in addition, it may indicate allosteric effect or proximity between GSH and CDNB binding sites in *Pf*GST.

With respect to hGSTP1, the random-ordered equation showed best fit to kinetic data. The deduced dissociation constants of $K^{GSH}$ and $K^{CDNB}$ were 0.14 and 0.4 mM, respectively. The $\propto$ factor was equal to 2.6 which indicates mutual inhibitory effect or closeness between GSH and CDNB binding sites. Therefore, first binding of either GSH or CDNB has some inhibitory effect on subsequent binding of the other substrate. This observation can be rationalized structurally if consideration been given to the H-site volume which is confined in hGSTP1 and wide in *Pf*GST. Yet, the inhibitory effect of first substrate binding is limited and mutual i.e. it is not complete and sequenced as in compulsory-ordered mechanism.

The mGSTM1 was observed to bind GSH and CDNB in random-ordered mechanism. The dissociation constants of $K^{GSH}$ and $K^{CDNB}$ deduced from the fitted equation were 0.3 and 0.2 mM, respectively. Unlike hGSTP1, the $\propto$ factor for mGSTM1 was less than one and indicate no mutual inhibition between the two substrates. Conclusively, larger distance between GSH and CDNB binding sites may characterize mGSTM1, yet not *Pf*GST and hGSTP1. The figures of fitting the equations to kinetic data are provided in Supplementary material, Figure II.

### 3.3. Determination of the modes for inhibitors binding, the affinities and the construction of molecular models

GSTs are bisubstrate enzymes in which the activity can be measured by the rate of GS-DNB formation. Inhibition of GST activity can be measured by $\boldsymbol{K_i^{GSH}}$ and $\boldsymbol{K_i^{CDNB}}$ constants which measure the inhibitor affinity toward GSH and CDNB binding sites, respectively. The $K_i$ value measures the ligand affinity toward the free enzyme molecule in presence of defined concentration of one substrate in mono-substrate enzymes, and two substrates in bi-substrate enzymes. In GSTs, the $K_m$ value of one substrate (e.g. CDNB) depends on the concentration of the other substrate (e.g. GSH). Therefore, measuring the $K_i$ value for an inhibitor in GSTs using Michaelis-Menten equation of mono-substrate gives inhibitor affinity toward enzyme-substrate complex and not free enzyme.

The cibacron blue (CB), ethacrynic acid (EA), hemin, and S-hexyl glutathione (GSX) are known GST inhibitors (Harwaldt et al., 2002; Liebau et al., 2005), of which glutathione scaffold (Adang et al., 1988; Adang et al., 1989; Adang et al., 1990; Adang et al., 1991; Meyer, 1993; McHugh et al., 1996; Chang et al., 1998; Burg et al., 2002a; Burg et al., 2002b; Cacciatore et al., 2005) and EA (Zhao et al., 2005; Zhao et al., 2006) were used as lead compounds. Using the standard GST assay, the binding mode and inhibition constants of $K_i^{GSH}$ and $K_i^{CDNB}$ as well as the interaction factor of apha were determined and summarized in Table 3. The fitting of equations to kinetic data and the double-reciprocal plots are provided in Supplementary material.

#### 3.3.1. Cibacron blue (CB)

CB is a ligand-in non-substrate inhibitor for GSTs. Due to its high affinity, the potential of using CB or its moieties as lead compounds for GST inhibitors is being investigated. The kinetic results (Supplementary material Figures IIIa–c) showed that CB inhibits *Pf*GST by competing both of GSH ($K_i^{GSH}$ = 0.25 μM) and CDNB ($K_i^{CDNB}$ = 0.3 μM). However, CB competes CDNB ($K_i^{CDNB}$ = 0.3 μM) but not GSH ($K_i^{GSH}$ = 0.21 μM) in hGSTP1 while CB not competing both substrates in mGSTM1 ($K_i^{GSH}$ = 2 μM, $K_i^{CDNB}$ = 2.6 μM).

The competition between CB and CDNB in hGSTP1 was consistent with the X-ray crystallographic structure of GS-DNB which overlaps with CB at the H-site (Oakley et al., 1999) (Fig.1). According to the electron density map for crystal structure of hGSTP1 in complex with cibacron blue (PDB ID 20GS), only the anthraquinone moiety of CB was visible and not disulphophenyl triazine (DSPT) moiety (Oakley et al., 1999). Docking of isolated anthraquinone moiety of CB back to hGSTP1 gave no poses which overlaps with the crystal conformation. However, docking the complete CB structure gave pose with the anthraquinone moiety nicely overlapped with the crystal conformation (Fig. 2). The

**Table 3**
The kinetic results for inhibition of PfGST, hGSTP1 and mGSTM1 by different ligands. The values are given as vector represents mode of inhibition, $K_i$, and alpha values.

| Inhibitor | Variable substrate | *Pf*GST | hGSTP1 | mGSTM1 |
|---|---|---|---|---|
| Cibacron blue | GSH | C,0.25 ± 0.02 μM | NC, 0.21 ± 0.03 μM, 1.4 ± 0.6 | NC, 2.0 ± 0.8 μM, 0.3 ± 0.15 |
| | CDNB | C, 0.3 ± 0.02 μM | C, 0.3 ± 0.02 μM | NC, 2.5 ± 1 μM, 0.26 ± 0.1 |
| Ethacrynic acid | GSH | NC, 21.4 ± 2.6 μM, 2.4 ± 0.5 | NC, 112 ± 21 μM, 0.36 ± 0.9 | UC, 6.6 ± 0.4 μM |
| | CDNB | C, 35 ± 2 μM | C, 8.8 ± 0.7 μM | NC, 0.7 ± 0.07 μM, 5.7 ± 0.8 |
| *S*-hexyl glutathione | GSH | C, 37.6 ± 2.2 μM | C, 51 ± 3 μM | C, 3.5 ± 0.14 μM |
| | CDNB | C, 120 ± 4 μM | NC, 42 ± 4 μM,1.2 ± 0.4 | NC, 3.17 μM, 4.6 |
| Hemin | GSH | NC, 0.43 ± 0.08 μM, 3.5 ± 1 | C, 2.5 ± 0.4 μM | NC, 1.5 ± 0.2 μM, 1 ± 0.2 |
| | CDNB | C, 0.6 ± 0.1 μM | C, 3.8 ± 0.3 μM | NC, 0.62 ± 0.16 μM, 3 ± 1 |
| Protoporphyrin ix | GSH | NC, 26 μM, 1 | C, >50 μM | NC, 7.3 ± 1.3 μM, 6.3 ± 2.8 |
| | CDNB | NC, 29 ± 8 μM, 0.28 ± 0.14 | C, >100 μM | NC, 35 ± 21 μM, 0.38 ± 0.26 |

Note: The inhibition is C = competitive, UC = uncompetitive, NC = non-competitive.

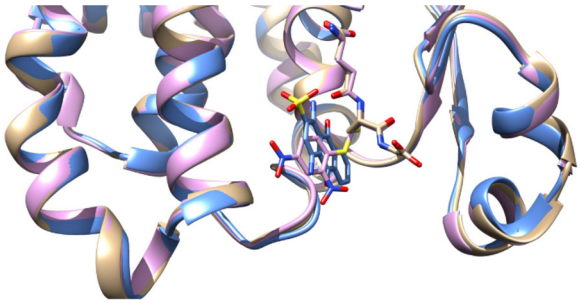

**Fig. 1.** Superimposed crystal structures of hGSTP1 in complex with GSH (PDB 8GSS, gold), GS-DNB (PDB 18GS, magenta), and cibacron blue (PDB 20GS, blue). The anthraquinone moiety of CB overlapped with CDNB but not with GSH binding sites. (For interpretation of the references to colour in this figure legend, the reader is referred to the web version of this article.)

estimated free energy of binding (EFEB) and $K_i$ were equal to −6.28 Kcal/Mol and 25 μM, respectively.

According to docking results the two sulfophenyl groups as well as the secondary amine of the triazine ring maintain three hydrogen bonds between DSPT moiety and the side chain hydroxyl group of Thr109. Both of the anthraquinone moiety and one of sulphophenyl rings are in hydrophobic interaction with Tyr108. According to crystal and docked conformations, the anthraquinone moiety interacts with residues from both of G and H-sites of hGSTP1. A hydrogen bond connects the ring carbonyl group of anthraquinone moiety to the hydroxyl group of Tyr7 while a salt bridge connects the sulfonic acid group of the moiety to the guanadyl group of Arg13. Moreover, 42 van der Waals interactions have been observed between the anthraquinone moiety and hGSTP1 (Oakley et al., 1999). However, our docking results reveal that the hydrogen bonds of the DSPT moiety efficiently stabilize the conformation of CB at H-site, which otherwise, cannot be attained by anthraquinone moiety alone.

Docking of CB to *Pf*GST revealed different binding mode compared to hGSTP1. The DSPT moiety of CB aligns at G-site of *Pf*GST and establishes five hydrogen bonds with Gln71 and Gln73 through the sulfophenyl and the secondary amino groups. While the anthraquinone moiety binds at the distal part of the thioredoxine domain (Fig. 2). Several inter-molecular hydrogen bonds and Van der Waals interactions stabilize the docked conformation of CB at thioredoxin domain of *Pf*GST to give EFEB of binding and $K_i$ values of −9.27 Kcal/Mol and 0.16 μM, respectively. The partial occupancy of *Pf*GST H-site by sulphophenyl group of docked CB may rationalize the experimentally observed competition with CDNB. For detailed interaction models for docked CB in hGSTP1 and *Pf*GST please see the Supplementary material Figures IV and V.

Docking of CB to mGSTM1 was not possible due to lack of crystal structure. Kinetically, about ten times lower affinity and different binding mode was observed for CB in mGSTM1 compared to *Pf*GST and hGSTP1. Thus, CB may bind away from G- and H-sites in mGSTM1.

The docked conformations of CB in hGSTP1 and *Pf*GST were further optimized via SZYBKI (from OpenEye) using molecular mechanics force field of MMFF94S and conjugated gradient. The final energy accounted for intermolecular electrostatic and Van der Waals interactions, as well as for solvent effect which was calculated according to Poisson-Boltzmann (PB) model. Flexibility has been permitted for protein side chains including the polar hydrogen atoms within 4 Å from CB. The intermolecular interaction energy determined by SZYBKI for CB in hGSTP1 was different than in *Pf*GST (−16 and −27 Kcal/Mol, respectively). According to the calculated energies (Table 4), DSPT moiety provides about half of the total electrostatic binding energy of CB in hGSTP1 and *Pf*GST. The kinetic results approved different binding mode in *Pf*GST where both of G and H-sites are occupied by CB. Due to the wide space in *Pf*GST between thioredoxin domain that contains G-site and C-terminal domain that contains H-site, large molecules like CB ($M_{wt}$ = 840) can find enough space to bind and block both sites. On the other hand, narrower space is available in hGSTP1 which can allow only for portion of the CB molecule (anthraquinone moiety) to bind (Oakley et al., 1999), while the rest of the molecule (i.e. DSPT moiety) maintains stabilizing H-bonds and Van der Waals interactions out of H-site toward C-terminal domain, as approved by docking experiments. Therefore, in spite of occupying the H-site of hGSTP1, the crystal structure of isolated anthraquinone moiety of CB may be inappropriate for structure-based analogues design. The requisite for DSPT moiety as well as the intrinsic toxicity (Sendelbach, 1989) render the isolated anthraquinone moiety an unsuitable scaffold for the design of hGSTP1

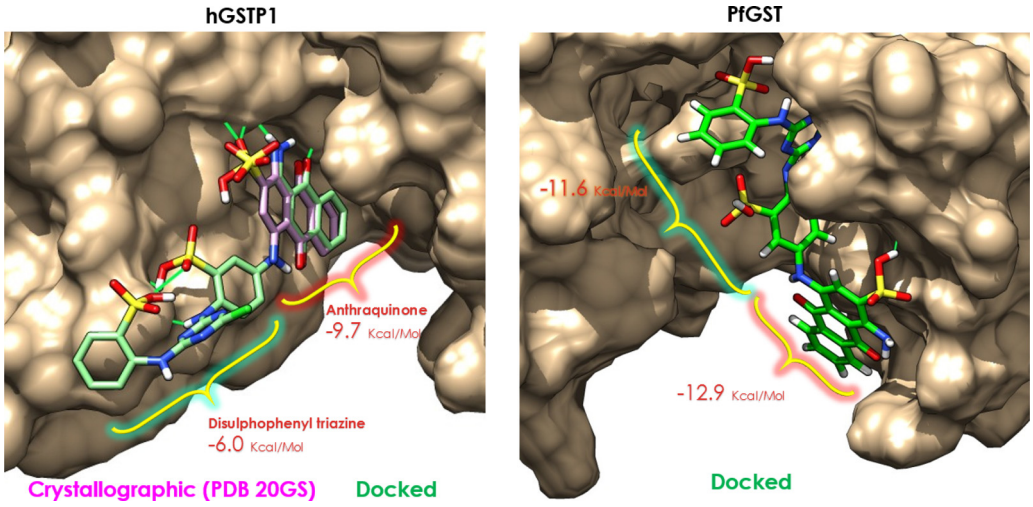


**Fig. 2.** The binding mode of docked cibacron blue (green) at the H and G-sites of hGSTP1 and PfGST, respectively. The docked and crystal conformations (magenta) of anthraquinone moiety of cibacron blue are overlapped in hGSTP1. The Inter-molecular H-bonds (green lines) and interaction energies (calculated by SZYBKI) for anthraquinone and disulphophenyl triazine moieties are shown. (For interpretation of the references to colour in this figure legend, the reader is referred to the web version of this article.)

**Table 4**
The intermolecular interaction energy terms as calculated by SZYBKI using MMFF94S with flexible protein side chains including flexible polar hydrogen atoms.

| | Energy in Kcal/Mol | hGSTP1 | *Pf*GST |
|---|---|---|---|
| Full cibacron | VdW | −12.22 | −23.78 |
| | Electrostatic (diel = 1.0) | −53.22 | −78.55 |
| | Protein desolv (PB) | 17.13 | 20.38 |
| | Ligand desolv (PB) | 15.20 | 19.46 |
| | Solvent screening (PB) | 17.49 | 37.14 |
| | **final** | **−15.62** | **−27.35** |
| Anthraquinone moiety | VdW | −11.38 | −10.17 |
| | Electrostatic (diel = 1.0) | −29.56 | −56.54 |
| | Protein desolv (PB) | 12.02 | 7.17 |
| | Ligand desolv (PB) | 7.41 | 6.79 |
| | Solvent screening (PB) | 11.85 | 39.83 |
| | **final** | **−9.66** | **−12.85** |
| DSPT moiety | VdW | −1.08 | −13.85 |
| | Electrostatic (diel = 1.0) | −24.01 | −40.42 |
| | Protein desolv (PB) | 5.37 | 12.414 |
| | Ligand desolv (PB) | 7.66 | 11.08 |
| | Solvent screening (PB) | 6.03 | 19.20 |
| | **final** | **−6.02** | **−11.57** |

inhibitors. Rational selection of CB moieties as scaffolds for designing *Pf*GST inhibitors as well as the subsequent modifications requisite structural determination of *Pf*GST-CB complex.

### 3.3.2. Ethacrynic acid (EA)

EA is substrate for GSTs that catalyze its conjugation to GSH (Ploemen et al., 1994; Oakley et al., 1997c). EA was considered as lead compound for GST inhibitors and used clinically to reduce cellular resistance to chemotherapy. According to kinetic results, EA binds the substrate binding site (H-site) and competes CDNB in *Pf*GST ($K_i^{CDNB}$ = 35 μM) and hGSTP1 ($K_i^{CDNB}$ = 21.4 μM). However, no competition with CDNB was observed in mGSTM1 which may indicate different binding sites for CDNB and EA in this isoform of GST. The observation in mGSTM1 can be considered as an application of "degeneracy" phenomenon in which different GST substrates occupy different sub-sites of the H-site (Mahajan and Atkins, 2005). On the other hand, consistent non-competitive inhibition was observed for EA toward GSH in all of *Pf*GST, hGSTP1, and mGSTM1, which indicates no G-site occupation. The inhibition plots are provided in Supplementary material (Figure VIa–c)

The crystal structure of free EA bound to hGSTP1 indicates the necessity of water molecules for mediating ligand-protein hydrogen bonds (Oakley et al., 1997c). Possibly because of relatively small molecular size and limited direct interactions with the protein, different binding modes were crystallographically observed for EA and its conjugate GS-EA in hGSTP1 (Oakley et al., 1997b). The difference in binding mode could be related to minor changes in crystallization conditions and/or technique used to introduce ligand molecule into protein crystal (crystal soak or co-crystallization) (Oakley et al., 1997b; Oakley et al., 1997c). Therefore, the crystallographically observed water molecules seem to be important in bridging hydrogen bonds between EA and hGSTP1 (Fig. 3). Consequently, molecular docking for both of EA and GS-EA against hGSTP1 was unsuccessful in reproducing the crystal conformations without using crystal water molecules. Similarly, docking against *Pf*GST did not give reliable results that satisfy the experimental kinetic data.

With respect to mGSTM1, EA inhibition was uncompetitive with GSH and non-competitive with CDNB. Therefore, EA can bind with higher stability to mGSTM1-GSH complex compared to empty enzyme, however, at site other than for CDNB. The enzyme may undergo structural changes after binding GSH which improves EA affinity or GSH may impart in formulation of EA binding site. The

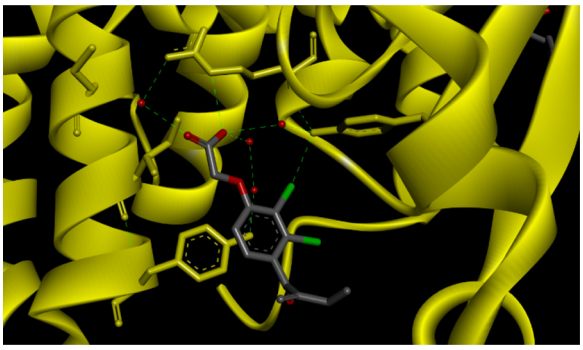

**Fig. 3.** The crystal structure of hGSTP1 in complex with EA (PDB 3GSS) showing oxygen atom of crystal water molecules (red spheres) which are involved in maintaining network of hydrogen bonds (green dashed lines) between ligand and the protein. (For interpretation of the references to colour in this figure legend, the reader is referred to the web version of this article.)

value of α factor of more than one for non-competitive CDNB inhibition, indicates tendency toward competition, i.e. possible proximity between CDNB and EA sub-sites within H-site of mGSTM1. Similarly, EA has higher affinity to hGSTP1-GSH complex ($K_i^{CDNB}$ = 21.4 μM) compared to hGSTP1-CDNB complex ($K_i^{GSH}$ = 112 μM), which was observed upon using stable 1 mM concentration of GSH and CDNB, respectively. The overall higher affinity of EA toward mGSTM1 compared to *Pf*GST and hGSTP1 is consistent with a previous report (Ploemen et al., 1993).

Both of EA and GS-EA conjugate are reversible inhibitors for GSTs, moreover, EA can inhibit GSTs by reversible covalent bonding (Ploemen et al., 1994). Therefore, the rational use of EA as lead compound for GST inhibitor design strongly depends on which form of EA is involved as well as the mechanism of inhibition (Please see Section 3.4 for details).

### 3.3.3. S-hexyl glutathione (GSX)

GSX is a *S*-hexyl conjugate of GSH that inhibit GSTs. GSX is considered a prototype of GSH conjugates developed to be used as GST inhibitors. The kinetic results showed that GSX inhibit *Pf*GST, hGSTP1 and mGSTM1 solely by competing GSH substrate ($K_i^{GSH}$ equals 37.6, 51 μM and 3.5 μM, respectively). On the other hand, GSX competition with CDNB is more obvious in *Pf*GST ($K_i^{CDNB}$ = 120 μM) compared to mGSTM1 ($K_i^{CDNB}$ = 3.17 μM, $\alpha$ = 4.6), while being almost non-competitive in hGSTP1 ($K_i^{CDNB}$ = 42.5 μM, $\propto$ = 1.2).

The kinetic results for GSX were consistent with X-ray crystallographic structures for hGSTP1 and *Pf*GST. According to crystallographic structures, the GSX binds hGSTP1 at the G-site sending its S-hexyl tail away from H-site toward the loop connecting β1 and α1 substructures of the thioredoxin domain (Fig. 4) (Oakley et al., 1997a). While in *Pf*GST, the S-hexyl tail adopts two conformations depending on multimeric state of the enzyme, however, both conformations pointed toward the H-site and diverged by an almost right angle (Perbandt et al., 2004; Hiller et al., 2006). Consequently, while no interaction is expected between GSX and CDNB in hGSTP1, competition is possible in *Pf*GST due to different directionality of S-hexyl tail. Unfortunately, no crystal structures are available neither for mGSTM1 nor for its close partner hGSTM1 in complex with GSX, however, our kinetic results suggest equivalent binding mode to hGSTP1. Higher affinity was observed for GSX toward mGSTM1 compared to the other isoforms. Inspite of peptidic nature and lower affinity, GSH conjugates are of earliest designed GSTs inhibitors and represent an application of product inhibition observed in GSTs (Meyer, 1993). Suggestions for design of GSH analouges as *Pf*GST inhibitors

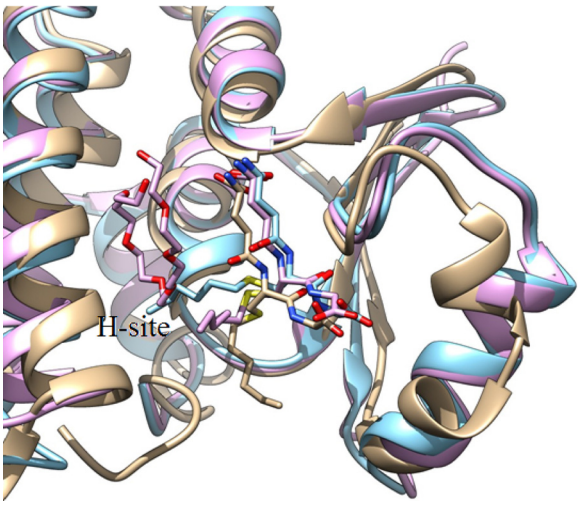


**Fig. 4.** Crystal structure of hGSTP1 with S-hexyl glutathione (PDB 9GSS, brown) superimposed on asymmetric unit cells for PfGST dimer (PDB 2AAW, magenta) and tetramer (PDB 1Q4J, cyan). The S-hexyl tail accommodates different orientation in each crystal. In hGSTP1, the tail is descending down toward the loop connecting β1 and α1 of thioredoxine domain. While in PfGST, the tail is directed toward the inner (cyan) or outer (magenta) sides of H-site. Note that PEG330 molecule occupied the H-site in 2AAW.

will be revisited in next sections. For inhibition plots, please see Supplementary material Figure VIIa–c).

### 3.3.4. Hemin and protoporphyrin IX (ProtoIX)

Similar to CB, hemin and ProtoIX are ligand-in, non-substrate competitive inhibitors for GSTs which were proposed to bind at H-site (Caccuri et al., 1990; Liebau et al., 2005). While the interaction of hemin to hGSTP1 and mGSTM1 has no medicinal application yet, the inhibition of hemin interaction to *Pf*GST is considered as anti-malarial target (Srivastava et al., 1999; Harwaldt et al., 2002). The kinetic results for *Pf*GST showed that hemin principally competes CDNB ($K_i^{CDNB} = 0.6\,\mu M$) and to some extent GSH ($K_i^{GSH} = 0.43$, $\alpha = 3.5$). In hGSTP1, hemin competition was observed at both of GSH ($K_i^{GSH} = 2.4\,\mu M$) and CDNB ($K_i^{CDNB} = 3.8\,\mu M$) binding sites. On the contrary, no competition was observed at GSH binding site in mGSTM1, however, with tenuous tendency toward CDNB binding site ($K_i^{GSH} = 1.5\,\mu M$, $\alpha = 1$ and $K_i^{CDNB} = 0.6\,\mu M$, $\alpha = 3$). Therefore, hemin may bind mGSTM1 at site away from G and H-sites (Vander Jagt et al., 1985).

Several reports suggested the existence of other binding sites in GSTs used for ligand-in binding. The sites are located at the dimer interface (McTigue et al., 1995; Ji et al., 1996) or at the back of the enzyme where HEPES or MES molecules bind (Ji et al., 1997; Prade et al., 1997; Perbandt et al., 2015). In hGSTP1, two binding sites were proposed to be available for binding hemin, where GSH enhances hemin binding to one site while inhibits binding to the second (Caccuri et al., 1990). However, CDNB binding site was not regarded as one of the two hemin binding sites in hGSTP1 as non-competitive inhibition was reported ($K_i^{CDNB} = 4\,\mu M$) (Caccuri et al., 1990). Similarly, *Pf*GST was reported to bind hemin with high and low affinity modes depending on presence and absence of GSH, respectively (Liebau et al., 2009).

In order to understand the mode of hemin interaction to GSTs, molecular docking was performed. Initial docking results of hemin in hGSTP1 suggests two binding sites for each monomer (A-site and B-site) as shown in Fig. 5. The A-site is overlapped with

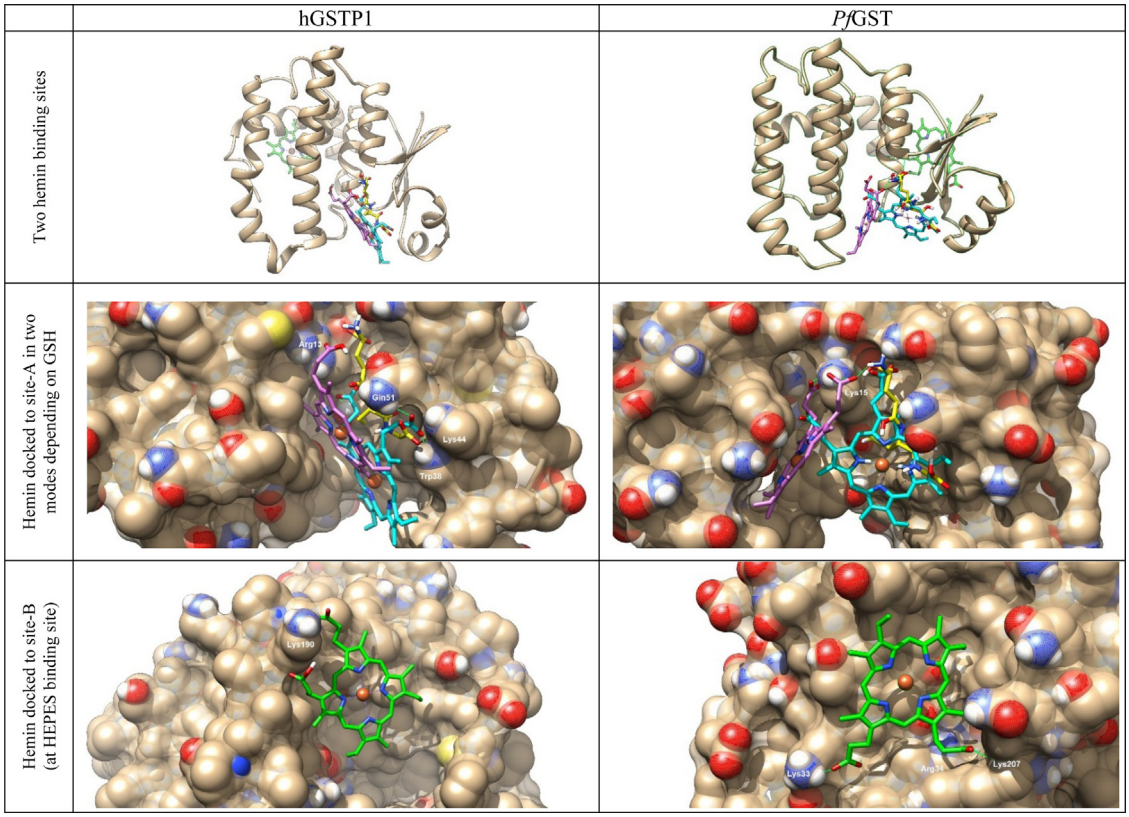


**Fig. 5.** The docking of hemin to hGSTP1 (left) and PfGST (right). Hemin docked toward site-A in absence (cyan) and presence (magenta) of GSH at G-site (yellow). Docking of hemin toward site-B (green) occurred at site equivalent to HEPES binding site. (For interpretation of the references to colour in this figure legend, the reader is referred to the web version of this article.)

substrate binding site (H-site), while B-site is located at the back of G-site between β2 and α1 which is equivalent to HEPES and MES binding site in hGSTP1 (Ji et al., 1997; Oakley et al., 1997a; Ji et al., 1999). Subsequently, molecular docking experiments using more extensive search parameters were performed on each site. Two possible binding modes for hemin were obtained at A-site depending on presence or absence of GSH at G-site. In the presence of GSH, the carboxylic group of hemin establishes hydrogen bond with α-amino group of γ-glutamyl residue of GSH. While in absence of GSH, hemin occupies part of the G-site. These

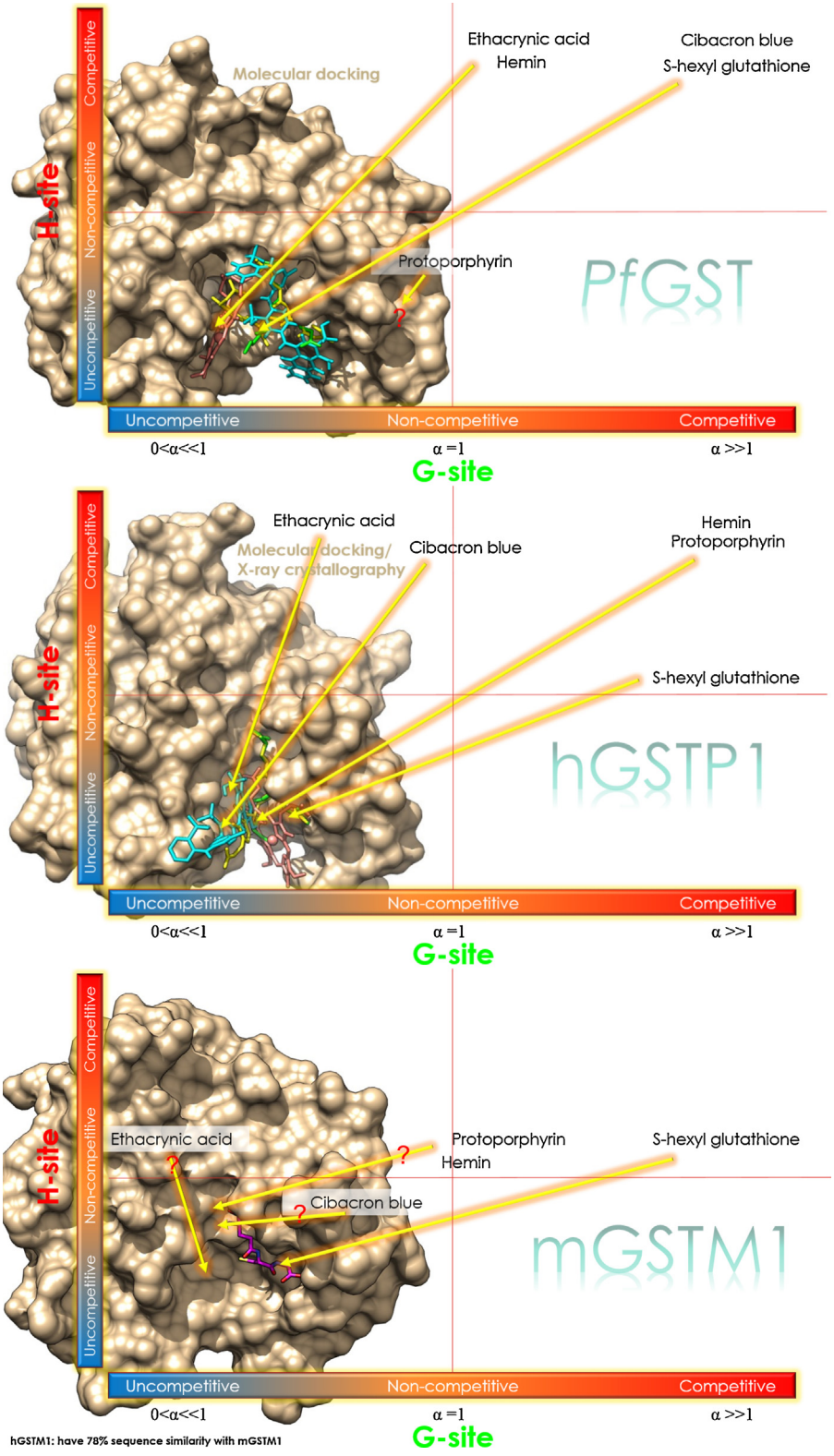


**Fig. 6.** Enzyme kinetic and molecular docking experiments cooperate to build the interaction models for GSX (green), CB (cyan), hemin (red), EA (yellow) at each of PfGST, hGSTP1 and mGSTM1. The crystal structure of hGSTM1 bound to GSH (pink) is shown instead of mGSTM1 (unavailable crystal structure). (For interpretation of the references to colour in this figure legend, the reader is referred to the web version of this article.)

predictions for hemin binding satisfy the kinetically observed competition with GSH and CDNB, a previously reported kinetic study (Caccuri et al., 1990), the none requirement for free GSH thiol group for hemin interaction (Caccuri et al., 1990), and a previously reported measurement of hemin-Cys47 distance (10–14 Å) by electron paramagnetic resonance (Desideri et al., 1991). Interestingly, the C-terminal tail in hGSTP1 which impart in H-site formation (Reinemer et al., 1992) has no direct interaction with hemin docked to B-site, and consequently, no allosteric effect is expected.

Similar to hGSTP1, hemin was docked to A and B-sites within *Pf*GST. The results indicate that in the presence of GSH at G-site, hemin binds at A-site between C-terminal of α4 and N-terminal of α1, as previously reported by Liebau et al. (2005). The two carboxylic groups of hemin establish hydrogen bonds with Lys15 as well as α-amino group of γ-glutamyl residue of GSH. While in absence of GSH, hemin occupies G-site and part of H-site. Comparing the values of EFEB for docked hemin showed that hemin affinity increased in presence of GSH (-9.58 Kcal/Mol with GSH) compared to empty G-site (–6.8 Kcal/Mol without GSH). The stabilization of hemin can best be described by un-competitive mode of interaction with GSH (Caccuri et al., 1990; Harwaldt et al., 2002), however, low competition was experimentally observed (interaction factor $\alpha = 3.5$). The kinetic and docking results agree with the reported prerequisite of G-site occupancy by GSH for optimum hemin binding (Harwaldt et al., 2002; Liebau et al., 2005; Liebau et al., 2009). The B-site for hemin docking in *Pf*GST was located between β2 and α1 (B-site). The two carboxylic groups of docked hemin are in hydrogen bonding interactions with main chain amino groups of Lys207 and Arg34. The distance between docked hemin at B-site and Trp131 (32 Å) was consistent with the previously calculated Förster distance (34 Å) (Liebau et al., 2005). Therefore, it is possible that hemin binding to B-site may allosterically affect substrate binding to H-site by steering the short C-terminal tail of the enzyme. According to intrinsic fluorescence quenching study, *Pf*GST binds hemin with high and low affinity modes depending on presence or absence of GSH, respectively. Yet, the ability of *Pf*GST-GSSG complex to bind hemin (Liebau et al., 2009) in spite of the possible clashes suggests the presence of another hemin binding site than the H-site.

The protoIX (which is equivalent to hemin, however, without Fe atom) showed lower affinity than hemin in all of *Pf*GST, hGSTP1, and mGSTM1. The modes of inhibitions with respect to both of GSH and CDNB substrates were non-competitive in *Pf*GST ($K_i^{GSH} = 26\ \mu M$, $\alpha = 1$ and $K_i^{CDNB} = 29\ \mu M$, $\alpha = 0.28$, respectively) and slight competitive in mGSTM1 ($K_i^{GSH} = 7.3\ \mu M$, $\alpha = 6.3$ and $K_i^{CDNB} = 35\ \mu M$, $\alpha = 0.4$, respectively). The hGSTP1 was resistant to inhibition by protoIX and the determination of $K_i$ values was difficult due to the interference with GS-DNB absorption at higher ProtoIX concentration. However, the observed $K_i$ values for protoIX in *Pf*GST were higher than the previously reported values (Harwaldt et al., 2002; Liebau et al., 2002).

In *Pf*GST, the Fe atom of docked hemin was far from establishing interaction with thiol group of GSH (Liebau et al., 2005) and within 5–7 Å from Tyr108, Asn111, Asn112, and Tyr211. However, possible interaction with Asn112 (Liebau et al., 2005) and water mediated hydrogen bonds may rationalize the impact of Fe atom in hemin binding. Therefore, lower affinity was observed for protoIX compared with its Ferrous partner (hemin). Nevertheless, the inhibitory mode of protoIX was similar to hemin with respect to GSH but not CDNB substrates (i.e. protoIX was unable to compete CDNB). This observation for protoIX may indicate potential change in binding mode to A-site in presence of GSH at G-site. Similarly, the lower affinity of protoIX toward hGSTP1 indicates the importance of Fe atom in hemin interaction. For inhibition plots, please see Supplementary material Figures VIIIa–c and IXa–c).

The overall summary for enzyme kinetics and molecular docking results for all ligands is provided in Fig. 6. Within the figure, the x and y axes were used to represent the range of α factor obtained from fitting non-competitive equation to fit kinetic data upon determination of $K_i^{GSH}$ and $K_i^{CDNB}$, respectively.

### 3.4. Interaction between different inhibitors at Pf*GST*

GSTs can bind to different type of molecules by different modes. Substrates of GSTs bind by productive mode to H-site, while non-substrates bind to any of the available sites without being catalyzed to product (Hayes et al., 2005; OAKLEY, 2011). While substrate molecules usually inhibit the conjugation activity competitively, the non-substrate molecules may do it non-competitively (Vander Jagt et al., 1985). Hemin is non-substrate for *Pf*GST, however it inhibits the conjugation activity by competing CDNB. Therefore both of CDNB and hemin may share similar binding site in *Pf*GST. Moreover, hemin may establish stabilizing interactions with GSH. Since dislodging of hemin from *Pf*GST is of medicinal application to combat heme buffering in the parasite (Harwaldt et al., 2002), the determination of ligands which compete hemin binding (whether being inhibitor for conjugation activity or not) is recommended for anti-malarial molecular design.

The interaction between *Pf*GST inhibitors of CB, EA, GSX and hemin have been studied using enzyme kinetics. The results indicate that inhibition of *Pf*GST by CB and GSX is not necessarily result in competition of hemin binding (Table 5). Nevertheless, CB enhances hemin binding to *Pf*GST ($\alpha < 1$), which may support the previously proposed docked conformations of CB (to G-site) and hemin (to H-site). GSX does not interact with hemin and the two inhibitors bind independently. In other word, the S-hexyl tail which was shown to compete CDNB, does not reach hemin binding site. However, EA was able to inhibit *Pf*GST as well as to compete hemin binding. Therefore, EA may share similar binding site with

**Table 5**
The dissociation constants and interaction factors obtained by fitting the kinetic data to previous equation. All experiments were performed at least in duplicates.

| Inhibitor i<br>Inhibitor j | Cibacron blue | Ethacrynic acid | *S*-hexyl glutathione |
|---|---|---|---|
| Ethacrynic acid | $K_i = 1.5$ $K_j = 53.3$<br>$\alpha$ = High ($1.34 \times 10^{17}$)<br>Competitive | | |
| S-hexyl glutathione | $K_i = 0.54$ $K_j = 87.9$<br>$\alpha = 100$<br>Competitive | $K_i = 50.5$ $K_j = 130.6$<br>$\alpha$ = High ($1.13 \times 10^{16}$)<br>Competitive | |
| Hemin | $K_i = 2.4$ $K_j = 4.4$<br>$\alpha = 0.37$<br>**Synergistic** | $K_i = 74.6$ $K_j = 4.8$<br>$\alpha$ = High ($1.38 \times 10^{20}$)<br>**Competitive** | $K_i = 155$ $K_j = 5.3$<br>$\alpha = 0.81$<br>**Independent** |

hemin. For inhibition plots, please see Supplementary material Figure X). Therefore, only EA competes hemin in *Pf*GST, while, CB, GSX, and CDNB compete EA but not hemin. Therefore, two suggestions can be provided to understand the mutual effect of EA. The first says that EA binding site may partially overlap on one side with hemin binding site and on the other side with the binding sites of CB, GSX, and CDNB. Accordingly, hemin has no direct contact with CB, GSX, and CDNB. The second suggestion depends on the observation that both of EA and its conjugate are GST inhibitors (Ploemen et al., 1993; Ploemen et al., 1994). Accordingly, the conjugated form of EA (GS-EA) is responsible for competing CB, GSX, and GS-DNB by its GS moiety, while competing hemin by its EA moiety.

In order to investigate whether EA conjugate (GS-EA) is responsible for hemin competition, two kinetic experiments were conducted to determine the $K_i^{GSH}$ and $K_i^{CDNB}$ for hemin using standard assay in the presence of 50 μM of EA. As expected, the previously observed non-competitive mode of inhibition for hemin toward GSH was changed to competitive mode in the presence of EA. In other word, increasing the concentration of GSH enhances the formation of GS-EA which produces direct competition to hemin. Therefore, at least the conjugated form of EA is responsible for inhibiting hemin binding to *Pf*GST. For inhibition plots, please see Supplementary material Figure XI).

Molecular simulations were performed to predict the binding mode of hemin competitors. The conjugated forms of EA (GS-EA) and CDNB (GS-DNB) have been created starting from crystal GSH moiety (PDB ID 2AAW). Subsequently, the Cartesian coordinates were optimized within *Pf*GST using SZYBKI to give the lowest energy conformations. The minimized conformation of GS-EA binds with total energy of −84 Kcal/Mol and the EA moiety of the conjugate is protruding toward the hemin binding site, thus, rationalizing the competition (Fig. 7). On the other hand, the minimized conformation of GS-DNB binds with total energy of −73 Kcal/Mol, however, it does not clash with hemin. Therefore, it is possible that the unconjugated form of CDNB was responsible for hemin competition.

Because of its low affinity, possibility of mediating few direct interactions with the protein, and the requirement for GSH conjugation to mediate hemin competition, EA may be unsuitable lead scaffold for hemin competitor. The S-substitution of GSH by flexible L-hexyl side chain may not necessarily compete hemin binding however, bulkier group may do. The observed improvement in hemin binding in presence of CB may indicate potential favorable interaction, which requires further study. A schematic summary of overall interaction model for *Pf*GST with GSH, GSX, CB, GS-EA, CDNB and hemin is provided in Fig. 8.

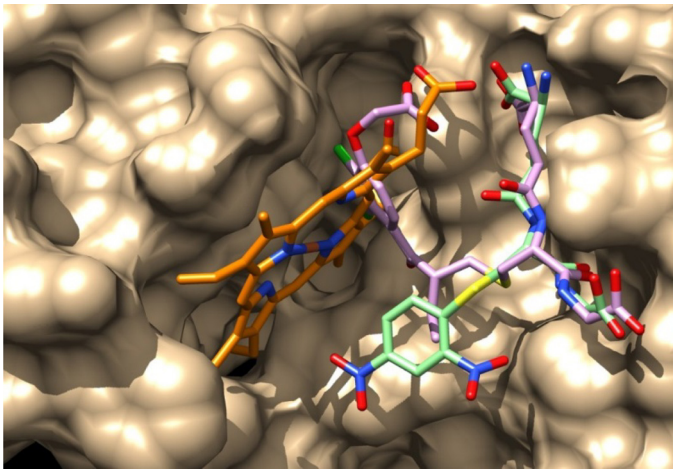

**Fig. 7.** Minimization of GS-EA (magenta) and GS-DNB (green) molecules within G and H-sites of PfGST. The docked conformation of hemin (orange) which is obtained in the presence of GSH at G-site is shown. (For interpretation of the references to colour in this figure legend, the reader is referred to the web version of this article.)

### 3.5. Hemin-HEPES interaction at PfGST

The 4-(2-hydroxyethyl)-1-piperazineethanesulfonic acid (HEPES, Fig. 9) was crystallographically observed bound to hGSTP1 at site other than G and H-sites (Ji et al., 1997). According to docking experiments, the secondary hemin binding site (B-site) is equivalent to HEPES binding site in hGSTP1. Similarly, docking showed that *Pf*GST binds HEPES at equivalent site between β2 and α1 (Fig. 9).

The *Pf*GST is the only known GST isoform that can coordinate into tetramer in absence of GSH (Tripathi et al., 2007). Hemin can bind to dimeric but not tetrameric form of *Pf*GST. Enough GSH is present in the parasite which enables stabilization of dimeric form of *Pf*GST even in oxidative state where GSSG dominates (Liebau et al., 2009). Similar effect was observed for HEPES to enhance the conversion of inactive *Pf*GST tetramer into active dimer. The effect is consistent with the observed lag phase at low GSH (Liebau et al., 2009) and/or HEPES concentrations. If both of HEPES and hemin share similar binding site in *Pf*GST, there will be an avenue for using HEPES scaffold in designing selective hemin competitors.

The kinetic results showed almost no inhibitory effect for HEPES (up to 200 mM) against *Pf*GST. In order to investigate possible interaction between hemin and HEPES at *Pf*GST binding sites, double inhibition kinetic experiment was performed using tetrameric form of *Pf*GST.

Pre-incubation of *Pf*GST tetramer with HEPES before initiating inhibitory assay by hemin provides kinetic data that fit to double inhibitor equation. The fitted equation provided dissociation constants for HEPES and hemin of 265 mM and 1.6 μM, respectively, and $\alpha$ interaction factor of 1.5. The high dissociation constant of HEPES indicate its weakness as *Pf*GST inhibitor if compared with hemin. The value of interaction factor close to unity indicates independent (non-competitive) binding of HEPES and hemin at *Pf*GST. Although it activates the dissociation of *Pf*GST

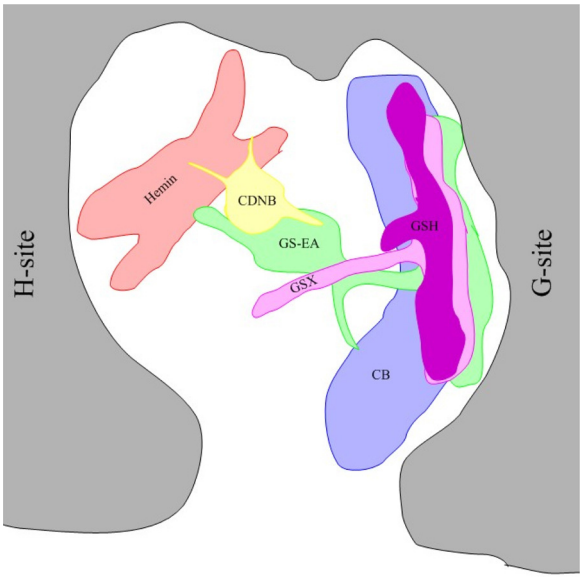


**Fig. 8.** Schematic representation of inhibitors binding in PfGST according to kinetic and docking results. The molecules are GSH (dark pink), CDNB (yellow), CB (blue), GSX (magenta), GS-EA (green), and hemin (red). (For interpretation of the references to colour in this figure legend, the reader is referred to the web version of this article.)

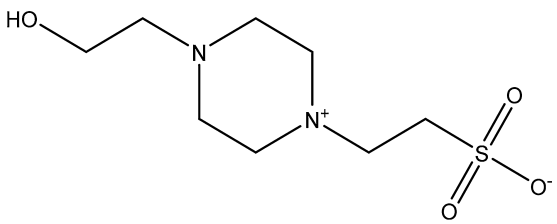


**Fig. 9.** Structure of 4-(2-hydroxyethyl)-1-piperazineethanesulfonic acid (HEPES).

tetramer (i.e. reduces the lag phase), HEPES reduces the activity of *Pf*GST dimer at higher concentrations without competing hemin at A-site. For inhibition plots, please see Supplementary material Figure XII).

Molecular docking experiment was conducted in order to structurally understand HEPES dynamics in term of *Pf*GST tetramer activation as well as possible antagonism of hemin binding at B-site. The results of docking against B-site of active *Pf*GST dimer (PDB 2AAW) showed that HEPES possibly competes hemin for binding (Fig. 10), yet, with lower affinity (EFEB = −2.8 Kcal/Mol, $K_i$ = 8.8 mM).The inactive tetrameric form of *Pf*GST is formed by stabilized interlock of two active dimers. For each monomer, the loop 113–119 from one dimer interlocks with part of the H-site from the other dimer (Hiller et al., 2006; Liebau et al., 2009) by a process which probably involves phosphate ions (Quesada-Soriano et al., 2014). According to docking results, HEPES may unlock the inactive tetrameric form of *Pf*GST by manipulating the interaction between C-terminal tail of one subunit and loop 113–119 of the other subunit. However, due to involvement of C-terminal tail in H-site formulation for *Pf*GST, high concentration of HEPES may inhibit substrate binding to *Pf*GST by allosteric effect. Although recent finding added controversy on the role of 113–119 loop in *Pf*GST tetramerization (Perbandt et al., 2015), it hinted to the existence of non-substrate binding site for 2-(N-morpholino) ethanesulfonic acid (MES) which is close to the site we proposed for HEPES. Both of HEPES and MES mediates hydrogen bonds to helix-8 main chain amide bonds (Fig. 10).

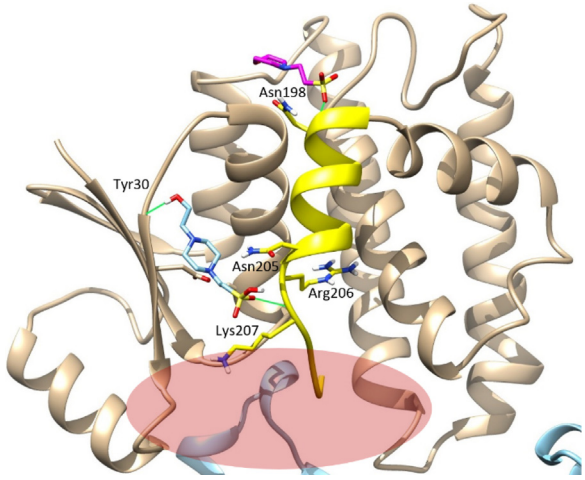


**Fig. 10.** The docked conformation of HEPES (blue stick) and crystal conformation of MES (magenta stick) interact with the helix 8 and the C-terminal tail of PfGST (yellow ribbon) through hydrogen bonds (green lines). The tetramer interlock (red oval) is possibly being steered by C-terminal tail. The tetramerization and MES binding site are shown by superimposing one unit of PfGST dimer (brown, PDB 2AAW) against the tetrameric form (cyan, PDB 1OKT) as well as PDB 4ZXG. (For interpretation of the references to colour in this figure legend, the reader is referred to the web version of this article.)

Although the competition between HEPES and hemin was suggested by docking experiment, it was not observed using enzyme kinetic experiment possibly due to lower affinity of HEPES. Therefore, further studies are required to judge whether HEPES scaffold can be used for designing hemin competitor in *Pf*GST.

## 4. Conclusions

The mechanisms of binding of GSH and CDNB substrates were kinetically determined by curve fitting to be compulsory-ordered in *Pf*GST while random-ordered in both of hGSTP1 and mGSTM1. The GST inhibitors were screened for lead scaffold able to compete hemin interaction to *Pf*GST. CB has higher affinity toward *Pf*GST and hGSTP1 compared to mGSTM1. CB has different binding modes in different GSTs and the isolated anthraquinone moiety may be unsuitable scaffold. EA has almost similar binding modes in *Pf*GST and hGSTP1, yet not in mGSTM1. At least EA conjugate (GS-EA) competes hemin in *Pf*GST. Low affinity of EA to *Pf*GST and involvement of water bridges renders the molecule unsuitable scaffold. GSX has lower affinity toward *Pf*GST and hGSTP1, compared to mGSTM1. The GSX and hemin binds *Pf*GST independently, thus, the S-hexyl tail is not approaching hemin binding site. Larger substitution at thiol or γ-amino group of γ-glutamine moiety may provide hemin competitor.

Hemin is non-substrate inhibitor for GSTs and competitively inhibit *Pf*GST at CDNB binding site, hGSTP1 at both of GSH and CDNB binding sites, while non-competitively inhibit mGSTM1. The Fe atom was shown to be important for hemin affinity compared to protoIX. Docking results showed that each of hemin and protoIX has two binding sites (A- and B- sites) in each of *Pf*GST and hGSTP1. The A-site is overlapped with H-site while B-site is overlapped with HEPES binding site. Binding of hemin and protoIX to A-site is improved by the presence of GSH at G-site. HEPES, which may involve in mediating tetrameric to dimeric transition in *Pf*GST, has low affinity ($K_d$ > 200 mM) and cannot compete with hemin binding. Accordingly, glutathione analogues with bulky substitution at thiol of cysteine moiety or at γ-amino group of γ-glutamine moiety represent promising leads for GST inhibitors with hemin competition. However, non-selectivity of glutathione analogues to *Pf*GST remains as another issue.

In absence of X-ray crystallographic data, the binding modes observed by kinetic experiments and predicted by molecular simulations can help to build ligand interaction models. The models can be used to address the capability of inhibitors to be lead scaffold for competing hemin buffering by *Pf*GST.

## Acknowledgements

Mohammed Nooraldeen Al-Qattan thanks Universiti Sains Malaysia for supporting his research by USM fellowship award. This research is funded by ERGS grant (Glutathione-S-transferase as a target for novel antimalarial compounds, No. 203/CDADAH/6730123). We are thankful for Dr. Becker research group at Universitat Giessen, at Institute of nutritional sciences, Biochemistry and Molecular Biology department for providing *Pf*GST encoded in protein expression vector. Thanks is given for free academic licenses from OpenEye (Openeye Toolkit), Chemaxon (Chemaxon for Excel and Chemaxon for office).

## Appendix A. Supplementary data

Supplementary data associated with this article can be found, in the online version, at http://dx.doi.org/10.1016/j.compbiolchem.2016.07.007.

## References


Adang, A.E., Duindam, A.J., Brussee, J., Mulder, G.J., Van Der Gen, A., 1988. Synthesis and nucleophilic reactivity of a series of glutathione analogues: modified at the gamma-glutamyl moiety. Biochem. J. 255, 715–720.

Adang, A.E., Meyer, D.J., Brussee, J., Van Der Gen, A., Ketterer, B., Mulder, G.J., 1989. Interaction of rat glutathione s-transferases 7-7 and 8-8 with gamma-glutamyl- or glycyl-modified glutathione analogues. Biochem. J. 264, 759–764.

Adang, A.E., Brussee, J., Van Der Gen, A., Mulder, G.J., 1990. The glutathione-binding site in glutathione s-transferases. Investigation of the cysteinyl: glycyl and gamma-glutamyl domains. Biochem. J. 269, 47–54.

Adang, A.E., Brussee, J., Van Der Gen, A., Mulder, G.J., 1991. Inhibition of rat liver glutathione s-transferase isoenzymes by peptides stabilized against degradation by gamma-glutamyl transpeptidase. J. Biol. Chem. 266, 830–836.

Adler, V., Yin, Z., Fuchs, S.Y., Benezra, M., Rosario, L., Tew, K.D., Pincus, M.R., Sardana, M., Henderson, C.J., Wolf, C.R., Davis, R.J., Ronai, Z., 1999. Regulation of jnk signaling by gstp. EMBO J. 18, 1321–1334.

Al-Qattan, M.N., Samian, M.R., Mordi, M.N., 2015. Cloning, heterologous expression and purification of glutathione-s-tranferases from human and mouse. Protein Expr. Purif..

Armstrong, R.N., 1991. Glutathione s-transferases: reaction mechanism structure, and function. Chem. Res. Toxicol. 4, 131–140.

Brophy, P.M., Barrett, J., 1990. Glutathione transferase in helminths. Parasitology 100 (Pt 2), 345–349.

Burg, D., Filippov, D.V., Hermanns, R., Van Der Marel, G.A., Van Boom, J.H., Mulder, G. J., 2002a. Peptidomimetic glutathione analogues as novel gammagt stable gst inhibitors. Bioorg. Med. Chem. 10, 195–205.

Burg, D., Hameetman, L., Filippov, D.V., Van Der Marel, G.A., Mulder, G.J., 2002b. Inhibition of glutathione s-transferase in rat hepatocytes by a glycine-tetrazole modified s-alkyl–gsh analogue. Bioorg. Med. Chem. Lett. 12, 1579–1582.

Cacciatore, I., Caccuri, A.M., Cocco, A., DE Maria, F., DI Stefano, A., Luisi, G., Pinnen, F., Ricci, G., Sozio, P., Turella, P., 2005. Potent isozyme-selective inhibition of human glutathione s-transferase a1-1 by a novel glutathione s-conjugate. Amino Acids 29, 255–261.

Caccuri, A.M., Aceto, A., Piemonte, F., DI Ilio, C., Rosato, N., Federici, G., 1990. Interaction of hemin with placental glutathione transferase. Eur. J. Biochem. 189, 493–497.

Chang, M., Zhang, F., Shen, L., Pauss, N., Alam, I., Van Breemen, R.B., Blond, S.Y., Bolton, J.L., 1998. Inhibition of glutathione s-transferase activity by the quinoid metabolites of equine estrogens. Chem. Res. Toxicol. 11, 758–765.

Cho, S.G., Lee, Y.H., Park, H.S., Ryoo, K., Kang, K.W., Park, J., Eom, S.J., Kim, M.J., Chang, T.S., Choi, S.Y., Shim, J., Kim, Y., Dong, M.S., Lee, M.J., Kim, S.G., Ichijo, H., Choi, E.J., 2001. Glutathione s-transferase mu modulates the stress-activated signals by suppressing apoptosis signal-regulating kinase 1. J. Biol. Chem. 276, 12749–12755.

Claro, E., 2000. Understanding initial velocity after the derivatives of progress curves. Biochem. Mol. Biol. Educ. 28, 304–306.

Copeland, R.A., 2000. Enzymes: A Practical Introduction to Structure, Mechanism, and Data Analysis. Wiley.com.

DE Luca, A., Federici, L., DE Canio, M., Stella, L., Caccuri, A.M., 2012. New insights into the mechanism of jnk1 inhibition by glutathione transferase p 1-1. Biochemistry 51, 7304–7312.

Danley, D.E., 2006. Crystallization to obtain protein-ligand complexes for structure-aided drug design. Acta Crystallogr. D Biol. Crystallogr. 62, 569–575.

Davis, A.M., St-Gallay, S.A., Kleywegt, G.J., 2008. Limitations and lessons in the use of x-ray structural information in drug design. Drug Discov. Today 13, 831–841.

Deharo, E., Barkan, D., Krugliak, M., Golenser, J., Ginsburg, H., 2003. Potentiation of the antimalarial action of chloroquine in rodent malaria by drugs known to reduce cellular glutathione levels. Biochem. Pharmacol. 66, 809–817.

Deponte, M., Becker, K., 2005. Glutathione s-transferase from malarial parasites: structural and functional aspects. In: Helmut, S., Lester, P. (Eds.), Methods in Enzymology. Academic Press.

Desideri, A., Caccuri, A.M., Polizio, F., Bastoni, R., Federici, G., 1991. Electron paramagnetic resonance identification of a highly reactive thiol group in the proximity of the catalytic site of human placenta glutathione transferase. J. Biol. Chem. 266, 2063–2066.

Egan, T.J., Combrinck, J.M., Egan, J., Hearne, G.R., Marques, H.M., Ntenteni, S., Sewell, B.T., Smith, P.J., Taylor, D., Van Schalkwyk, D.A., Walden, J.C., 2002. Fate of haem iron in the malaria parasite plasmodium falciparum. Biochem. J. 365, 343–347.

Fatumo, S., Plaimas, K., Mallm, J.P., Schramm, G., Adebiyi, E., Oswald, M., Eils, R., Konig, R., 2009. Estimating novel potential drug targets of plasmodium falciparum by analysing the metabolic network of knock-out strains in silico. Infect. Genet. Evol. 9, 351–358.

Federici, L., LO Sterzo, C., Pezzola, S., DI Matteo, A., Scaloni, F., Federici, G., Caccuri, A. M., 2009. Structural basis for the binding of the anticancer compound 6-(7-nitro-2,1,3-benzoxadiazol-4-ylthio)hexanol to human glutathione s-transferases. Cancer Res. 69, 8025–8034.

Fritz-Wolf, K., Becker, A., Rahlfs, S., Harwaldt, P., Schirmer, R.H., Kabsch, W., Becker, K., 2003. X-ray structure of glutathione s-transferase from the malarial parasite plasmodium falciparum. Proc. Natl. Acad. Sci. U. S. A. 100, 13821–13826.

Frova, C., 2006. Glutathione transferases in the genomics era: new insights and perspectives. Biomol. Eng. 23, 149–169.

Habig, W.H., Pabst, M.J., Jakoby, W.B., 1974. Glutathione s-transferases: the first enzymatic step in mercapturic acid formation. J. Biol. Chem. 249, 7130–7139.

Harwaldt, P., Becker, K., Rahlfsa, S., 2002. Glutathione s-transferase of the malarial parasite plasmodium falciparum: characterization of a potential drug target. Biol. Chem. 383, 821–830.

Hayes, J.D., Flanagan, J.U., Jowsey, I.R., 2005. Glutathione transferases. Annu. Rev. Pharmacol. Toxicol. 45, 51–88.

Hiller, N., Fritz-Wolf, K., Deponte, M., Wende, W., Zimmermann, H., Becker, K., 2006. Plasmodium falciparum glutathione s-transferase–structural and mechanistic studies on ligand binding and enzyme inhibition. Protein Sci. 15, 281–289.

Huang, Y.C., Misquitta, S., Blond, S.Y., Adams, E., Colman, R.F., 2008. Catalytically active monomer of glutathione s-transferase pi and key residues involved in the electrostatic interaction between subunits. J. Biol. Chem. 283, 32880–32888.

Huey, R., Morris, G.M., Olson, A.J., Goodsell, D.S., 2007. A semiempirical free energy force field with charge-based desolvation. J. Comput. Chem. 28, 1145–1152.

Huthmacher, C., Hoppe, A., Bulik, S., Holzhutter, H.G., 2010. Antimalarial drug targets in plasmodium falciparum predicted by stage-specific metabolic network analysis. BMC Syst. Biol. 4, 120.

Ivanetich, K.M., Goold, R.D., 1989. A rapid equilibrium random sequential bi-bi mechanism for human placental glutathione s-transferase. Biochim. Biophys. Acta 998, 7–13.

Ivanetich, K.M., Goold, R.D., Sikakana, C.N.T., 1990. Explanation of the non-hyperbolic kinetics of the glutathione s-transferases by the simplest steady-state random sequential bi bi mechanism. Biochem. Pharmacol. 39, 1999–2004.

Jakobson, I., Warholm, M., Mannervik, B., 1979. Multiple inhibition of glutathione s-transferase a from rat liver by glutathione derivatives: kinetic analysis supporting a steady-state random sequential mechanism. Biochem. J. 177, 861–868.

Ji, X., Von Rosenvinge, E.C., Johnson, W.W., Armstrong, R.N., Gilliland, G.L., 1996. Location of a potential transport binding site in a sigma class glutathione transferase by x-ray crystallography. Proc. Natl. Acad. Sci. U. S. A. 93, 8208–8213.

Ji, X., Tordova, M., O'donnell, R., Parsons, J.F., Hayden, J.B., Gilliland, G.L., Zimniak, P., 1997. Structure and function of the xenobiotic substrate-binding site and location of a potential non-substrate-binding site in a class pi glutathione s-transferase. Biochemistry 36, 9690–9702.

Ji, X., Blaszczyk, J., Xiao, B., O'donnell, R., Hu, X., Herzog, C., Singh, S.V., Zimniak, P., 1999. Structure and function of residue 104 and water molecules in the xenobiotic substrate-binding site in human glutathione s-transferase p 1-1. Biochemistry 38, 10231–10238.

Kalinina, E.V., Berozov, T.T., Shtil, A.A., Chernov, N.N., Glasunova, V.A., Novichkova, M.D., Nurmuradov, N.K., 2012. Expression of genes of glutathione transferase isoforms gstp 1-1 gsta4-4, and gstk1-1 in tumor cells during the formation of drug resistance to cisplatin. Bull. Exp. Biol. Med. 154, 64–67.

Laborde, E., 2010. Glutathione transferases as mediators of signaling pathways involved in cell proliferation and cell death. Cell Death Differ. 17, 1373–1380.

Leskovac, V., 2003. Comprehensive Enzyme Kinetics. Springer.

Liebau, E., Bergmann, B., Campbell, A.M., Teesdale-Spittle, P., Brophy, P.M., Luersen, K., Walter, R.D., 2002. The glutathione s-transferase from *Plasmodium falciparum*. Mol. Biochem. Parasitol. 124, 85–90.

Liebau, E., DE Maria, F., Burmeister, C., Perbandt, M., Turella, P., Antonini, G., Federici, G., Giansanti, F., Stella, L., LO Bello, M., Caccuri, A.M., Ricci, G., 2005. Cooperativity and pseudo-cooperativity in the glutathione s-transferase from plasmodium falciparum. J. Biol. Chem. 280, 26121–26128.

Liebau, E., Dawood, K.F., Fabrini, R., Fischer-Riepe, L., Perbandt, M., Stella, L., Pedersen, J.Z., Bocedi, A., Petrarca, P., Federici, G., Ricci, G., 2009. Tetramerization and cooperativity in plasmodium falciparum glutathione s-transferase are mediated by atypic loop 113–119. J. Biol. Chem. 284, 22133–22139.

Lisewski, A.M., Quiros, J.P., Ng, C.L., Adikesavan, A.K., Miura, K., Putluri, N., Eastman, R.T., Scanfeld, D., Regenbogen, S.J., Altenhofen, L., Llinas, M., Sreekumar, A., Long, C., Fidock, D.A., Lichtarge, O., 2014. Supergenomic network compression and the discovery of exp1 as a glutathione transferase inhibited by artesunate. Cell 158, 916–928.

Mahajan, S., Atkins, W.M., 2005. The chemistry and biology of inhibitors and pro-drugs targeted to glutathione s-transferases. Cell. Mol. Life Sci. 62, 1221–1233.

Mannervik, B., Board, P.G., Hayes, J.D., Listowsky, I., Pearson, W.R., 2005. Nomenclature for mammalian soluble glutathione transferases. Methods Enzymol. 401, 1–8.

Manoharan, T.H., Gulick, A.M., Puchalski, R.B., Servais, A.L., Fahl, W.E., 1992. Structural studies on human glutathione s-transferase pi: substitution mutations to determine amino acids necessary for binding glutathione. J. Biol. Chem. 267, 18940–18945.

Mchugh, T.E., Atkins, W.M., Racha, J.K., Kunze, K.L., Eaton, D.L., 1996. Binding of the aflatoxin-glutathione conjugate to mouse glutathione s-transferase a3-3 is saturated at only one ligand per dimer. J. Biol. Chem. 271, 27470–27474.

McTigue, M.A., Williams, D.R., Tainer, J.A., 1995. Crystal structures of a schistosomal drug and vaccine target: glutathione s-transferase from schistosoma japonica and its complex with the leading antischistosomal drug praziquantel. J. Mol. Biol. 246, 21–27.

Medh, R.D., Saxena, M., Singhal, S.S., Ahmad, H., Awasthi, Y.C., 1991. Characterization of a novel glutathione s-transferase isoenzyme from mouse lung and liver having structural similarity to rat glutathione s-transferase 8-8. Biochem. J. 278 (Pt 3), 793–799.

Meyer, D.J., 1993. Significance of an unusually low km for glutathione in glutathione transferases of the alpha mu and pi classes. Xenobiotica 23, 823–834.

Nebert, D.W., Vasiliou, V., 2004. Analysis of the glutathione s-transferase (gst) gene family. Hum. Genomics 1, 460–464.

OAKLEY, 2011. Glutathione transferases: a structural perspective. Drug Metab. Rev. 43, 138–151.

Oakley, A.J., Bello, M.L., Battistoni, A., Ricci, G., Rossjohn, J., Villar, H.O., Parker, M.W., 1997a. The structures of human glutathione transferase p 1-1 in complex with glutathione and various inhibitors at high resolution. J. Mol. Biol. 274, 84–100.
Oakley, A.J., LO Bello, M., Mazzetti, A.P., Federici, G., Parker, M.W., 1997b. The glutathione conjugate of ethacrynic acid can bind to human pi class glutathione transferase p 1-1 in two different modes. FEBS Lett. 419, 32–36.
Oakley, A.J., Rossjohn, J., Lo Bello, M., Caccuri, A.M., Federici, G., Parker, M.W., 1997c. The three-dimensional structure of the human pi class glutathione transferase p 1-1 in complex with the inhibitor ethacrynic acid and its glutathione conjugate. Biochemistry 36, 576–585.
Oakley, A.J., LO Bello, M., Nuccetelli, M., Mazzetti, A.P., Parker, M.W., 1999. The ligandin (non-substrate) binding site of human pi class glutathione transferase is located in the electrophile binding site (h-site). J. Mol. Biol. 291, 913–926.
Parker, L.J., Ciccone, S., Italiano, L.C., Primavera, A., Oakley, A.J., Morton, C.J., Hancock, N.C., Bello, M.L., Parker, M.W., 2008. The anti-cancer drug chlorambucil as a substrate for the human polymorphic enzyme glutathione transferase p1-1: kinetic properties and crystallographic characterisation of allelic variants. J. Mol. Biol. 380, 131–144.
Parker, L.J., Italiano, L.C., Morton, C.J., Hancock, N.C., Ascher, D.B., Aitken, J.B., Harris, H.H., Campomanes, P., Rothlisberger, U., DE Luca, A., LO Bello, M., Ang, W.H., Dyson, P.J., Parker, M.W., 2011. Studies of glutathione transferase p 1-1 bound to a platinum(iv)-based anticancer compound reveal the molecular basis of its activation. Chemistry (Easton) 17, 7806–7816.
Patskovsky, Y.V., Patskovska, L.N., Listowsky, I., 1999. Functions of his107 in the catalytic mechanism of human glutathione s-transferase hgstm1a-1a. Biochemistry 38, 1193–1202.
Patskovsky, Y.V., Patskovska, L.N., Listowsky, I., 2000. The enhanced affinity for thiolate anion and activation of enzyme-bound glutathione is governed by an arginine residue of human mu class glutathione s-transferases. J. Biol. Chem. 275, 3296–3304.
Perbandt, M., Burmeister, C., Walter, R.D., Betzel, C., Liebau, E., 2004. Native and inhibited structure of a mu class-related glutathione s-transferase from plasmodium falciparum. J. Biol. Chem. 279, 1336–1342.
Perbandt, M., Eberle, R., Fischer-Riepe, L., Cang, H., Liebau, E., Betzel, C., 2015. High resolution structures of plasmodium falciparum gst complexes provide novel insights into the dimer–tetramer transition and a novel ligand-binding site. J. Struct. Biol. 191, 365–375.
Pickett, C.B., Lu, A.Y., 1989. Glutathione s-transferases: gene structure, regulation, and biological function. Annu. Rev. Biochem. 58, 743–764.
Ploemen, J.H., Van Ommen, B., Bogaards, J.J., Van Bladeren, P.J., 1993. Ethacrynic acid and its glutathione conjugate as inhibitors of glutathione s-transferases. Xenobiotica 23, 913–923.
Ploemen, J.H., Van Schanke, A., Van Ommen, B., Van Bladeren, P.J., 1994. Reversible conjugation of ethacrynic acid with glutathione and human glutathione s-transferase p 1-1. Cancer Res. 54, 915–919.
Prade, L., Huber, R., Manoharan, T.H., Fahl, W.E., Reuter, W., 1997. Structures of class pi glutathione s-transferase from human placenta in complex with substrate: transition-state analogue and inhibitor. Structure 5, 1287–1295.
Quesada-Soriano, I., Barón, C., Téllez-Sanz, R., García-Maroto, F., García-Fuentes, L., 2014. Asn112 in plasmodium falciparum glutathione s-transferase is essential for induced reversible tetramerization by phosphate or pyrophosphate. Biochim. Biophys. Acta 1844, 1427–1436.
Reinemer, P., Dirr, H.W., Ladenstein, R., Huber, R., LO Bello, M., Federici, G., Parker, M. W., 1992. Three-dimensional structure of class pi glutathione s-transferase from human placenta in complex with s-hexylglutathione at 2.8 a resolution. J. Mol. Biol. 227, 214–226.
Ruzza, P., Rosato, A., Rossi, C.R., Floreani, M., Quintieri, L., 2009. Glutathione transferases as targets for cancer therapy. Anticancer Agents Med. Chem. 9, 763–777.
Schramm, V.L., Mccluskey, R., Emig, F.A., Litwack, G., 1984. Kinetic studies and active site-binding properties of glutathione s-transferase using spin-labeled glutathione a product analogue. J. Biol. Chem. 259, 714–722.
Sendelbach, L.E., 1989. A review of the toxicity and carcinogenicity of anthraquinone derivatives. Toxicology 57, 227–240.
Srivastava, P., Puri, S.K., Kamboj, K.K., Pandey, V.C., 1999. Glutathione-s-transferase activity in malarial parasites. Trop. Med. Int. Health 4, 251–254.
Townsend, D.M., Tew, K.D., 2003. The role of glutathione-s-transferase in anti-cancer drug resistance. Oncogene 22, 7369–7375.
Townsend, D.M., Findlay, V.L., Tew, K.D., 2005. Glutathione s-transferases as regulators of kinase pathways and anticancer drug targets. Methods Enzymol. 401, 287–307.
Townsend, D.M., 2007. S-glutathionylation: Indicator of cell stress and regulator of the unfolded protein response. Mol. Interv. 7, 313–324.
Tripathi, T., Rahlfs, S., Becker, K., Bhakuni, V., 2007. Glutathione mediated regulation of oligomeric structure and functional activity of plasmodium falciparum glutathione s-transferase. BMC Struct. Biol. 7, 67.
Vander Jagt, D.L., Hunsaker, L.A., Garcia, K.B., Royer, R.E., 1985. Isolation and characterization of the multiple glutathione s-transferases from human liver: evidence for unique heme-binding sites. J. Biol. Chem. 260, 11603–11610.
Zhao, G., YU, T., Wang, R., Wang, X., Jing, Y., 2005. Synthesis and structure-activity relationship of ethacrynic acid analogues on glutathione-s-transferase p 1-1 activity inhibition. Bioorg. Med. Chem. 13, 4056–4062.
Zhao, L., Huang, W., Liu, H., Wang, L., Zhong, W., Xiao, J., HU, Y., LI, S., 2006. Fk506-binding protein ligands: structure-based design, synthesis, and neurotrophic/neuroprotective properties of substituted 5,5-dimethyl-2-(4-thiazolidine) carboxylates. J. Med. Chem. 49, 4059–4071.
Zimniak, P., Nanduri, B., Pikula, S., Bandorowicz-Pikula, J., Singhal, S.S., Srivastava, S. K., Awasthi, S., Awasthi, Y.C., 1994. Naturally occurring human glutathione s-transferase gstp 1-1 isoforms with isoleucine and valine in position 104 differ in enzymic properties. Eur. J. Biochem. 224, 893–899.